FULL TITLE
ASP Conference Series, Vol. **VOLUME**, **YEAR OF PUBLICATION**
NAMES OF EDITORS

The Lockman Hole multi-wavelength survey

E. Rovilos, V. Burwitz, N. Bouché, S. Berta, D. Lutz, R. Genzel

Max Planck Institut für extraterrestrische Physik, Giessenbachstraße, 85748 Garching, Germany

G. Szokoly

MPE & Institute of Physics, Eötvös University, Pázmány P. s. 1/A, 1117 Budapest, Hungary

G. Hasinger, M. Salvato

Max Planck Institut für Plasmaphysik, Boltzmannstraße 2, 85748, Garching, Germany

E. Egami

Steward Observatory, University of Arizona, 933 North Cherry Avenue, Tucson, AZ 85721, USA

Abstract. We used the large binocular camera (LBC) mounted on the large binocular telescope (LBT) to observe the Lockman Hole in the U, B, and V bands. Our observations cover an area of 900 arcmin^2. We reached depths of 26.7, 26.3, and 26.3mag(AB) in the three bands, respectively, in terms of 50% source detection efficiency. We extracted a large number of sources ($\sim$ 89000), detected in all three bands and examined their surface density, comparing it with models of galaxy evolution. We find good agreement with previous claims of a steep faint-end slope of the luminosity functions, caused by late-type and irregular galaxies at $z > 1.5$. A population of dwarf star-forming galaxies at $1.5 < z < 2.5$ is needed to explain the U-band number counts. We also find evidence of strong supernova feedback at high redshift.

1. Introduction

The Lockman Hole is a region in the northern sky with minimal galactic absorption ($N_{\rm HI} = 4.5 \times 10^{19}$ cm^{-2}, Lockman, Jahoda & McCammon 1986) and the absolute minimum of infrared cirrus emission in the sky. As a result it is an ideal location for deep surveys. Indeed it has a large multi-wavelength coverage spanning from X-rays to meter-wavelength radio. In X-rays it has been observed with the ROSAT satellite (Hasinger et al. 1998) and more recently with XMM (Hasinger et al. 2001; Brunner et al. 2008), reaching a depth of 1.9×10^{-16} erg cm^{-2} s^{-1} in the 0.5-2.0 keV band. In the ultra-violet it has been observed by GALEX (Martin et al. 2005) as one of its deep fields, with the data being publically available. In the near infrared (J and K bands) it is a part of the UKIDSS ultra deep survey (Lawrence et al. 2007) reaching K$\sim$23(AB). In infrared wavelengths it was observed by ISO using both ISOPHOT and ISOCAM (Kawara et al. 2004; Fadda et al. 2004; Rodighiero et al. 2004) and more recently

there have been observations with Spitzer-IRAC (Huang et al. 2004) and Spitzer MIPS (Egami et al. 2008). The Lockman Hole is also part of the SWIRE survey (Lonsdale et al. 2003), observed with both IRAC and MIPS and covering a much wider (but shallower) area. There have been a number of millimeter - sub-mm observations of the Lockman Hole, namely with the JCMT-SCUBA (Coppin et al. 2006), JCMT-AzTEC (Scott et al. 2006), IRAM-MAMBO (Greve et al. 2004), and CSO-Bolocam (Laurent et al. 2005). In the radio regime, the Lockman Hole has been observed with the VLA, both in 5 and in 1.4 GHz (Ciliegi et al. 2003; Ivison et al. 2002; Biggs & Ivison 2006) and with MERLIN in 1.4 GHz (Biggs & Ivison 2008). Finally, in meter-wavelengths it was targeted by the GMRT (Garn et al. 2008).

2. LBT U-B-V observations

We observed the Lockman Hole with the Large Binocular Camera (LBC Giallongo et al. 2008) mounted on the Large Binocular Telescope (LBT) on Mount Graham, Arizona. The LBT has two 8.4 m diameter mirrors on a common mount, both of them equipped with a prime-focus camera. Both cameras have an 8 position filter wheel, ant there are 13 available filters, ranging from the ultraviolet to the near-infrared. For the Lockman Hole observations we used the LBT-Uspec filter, which is a U-band filter with more uniform wavelength coverage than the U-Bessel, and standard B and V-Bessel filters.

We observed the Lockman Hole during 24 observing runs, from February 2007 to March 2009. We spent a total of 36.8 hours on source with a 65% good data efficiency. The final integration time for the U, B, and V filters is 13.8, 5.55, and 5.35 hours respectively. We centred our imaging at the fields with deep XMM and VLA coverage (Hasinger et al. 2001; Ivison et al. 2002). These fields are separated by 8.6 arcmin, having a width of $\sim$ 10 arcmin (radius), so there is a large area of overlap, where our survey has the highest exposure time (see Fig. 1, right panel). The total area covered with the LBT is 900 arcmin^2.

For the data reduction we used the mscred package in IRAF, which is designed for the reduction of mosaic data. Special care was taken for the astrometry, because a prime-focus camera can introduce severe distortions. We have used the USNO-A2 (Monet 1998) catalogue to calibrate the astrometry, and have adopted a 4th order polynomial fit in both directions to compensate for the distortions. The final internal astrometric accuracy is 0.066 arcsec and relative to USNO-A2 it is 0.2 arcsec. The claimed accuracy of USNO-A2 is 0.25 arcsec.

3. Colours

In order to measure the colours of the sources in the Lockman Hole field we use a combination of the three images to detect sources and the individual images to measure their fluxes. As combination we use the "χ^2-image", which is the square root of the sum of the squares of the three images after scaling them to the same noise level. The $U-B$ vs. $B-V$ colours of the sources can be seen in Fig. 2. We compare the colours with colour tracks created from SED templates of different types of galaxies. In Fig. 2(left) we use the Coleman, Wu & Weedman (1980) templates and see that the bulk of the Lockman Hole sources are compatible with spiral or elliptical templates.

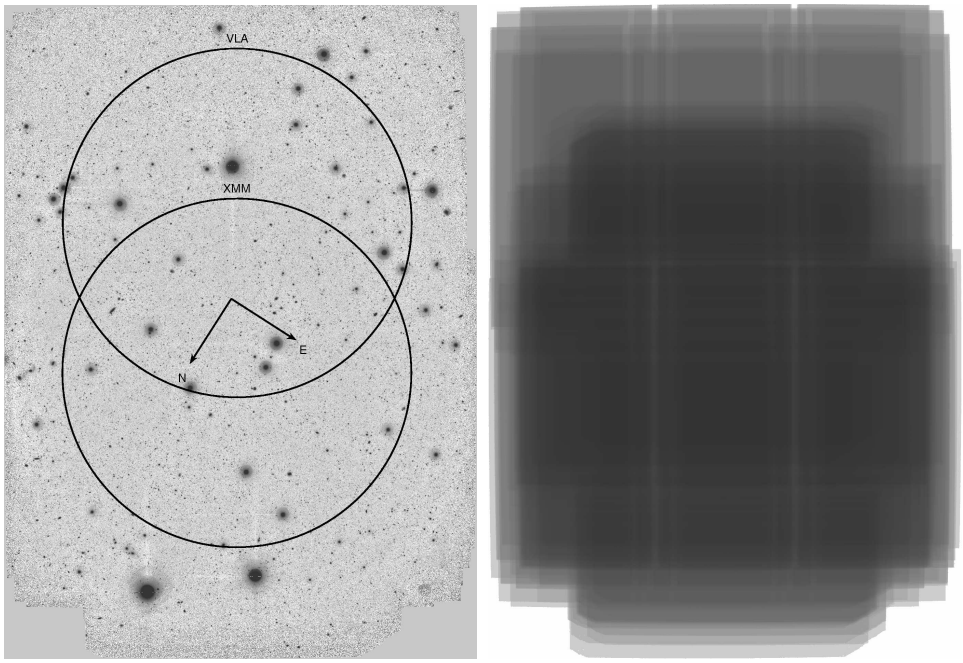

Figure 1. Final U-band image and corresponding exposure map. The image covers both the XMM and the VLA fields circular regions with the highest exposure in the area between them.

In Fig. 2(right) we use templates created with the GISSEL98 code (Bruzual & Charlot 1993) for different types of galaxies and varying stellar ages, metallicities and extinctions. We colour-code the tracks according to the redshift and we see that the redshifts better probed with this sample are in the range $0.5 \lesssim z \lesssim 2.5$. The region in the upper left corner of the image bracketed with the black line marks the "U-dropout" region with $z > 3$.

4. Number counts

In order to estimate the number count distributions in the *U*, *B*, and *V* bands we choose a region in the centre of the field where the sensitivity is uniform. We then run Monte-Carlo simulations in the three images separately using simulated sources in order to estimate the source detecting efficiency with respect to the magnitude of the source. This way we determine the sensitivity of the survey , which is 26.7, 26.3, and 26.3 mag(AB) for the *U*, *B*, and *V* bands respectively, in terms of 50% source detection efficiency.

The number count distributions we derived are plotted in red dots in Figs 3 and 4. Using the five faintest points of each distribution we calculate the faint-end slopes of the luminosity functions, which is -1.733 ± 0.018, -1.748 ± 0.006, and -1.507 ± 0.018 for the *U*, *B*, and *V* filters respectively. In Fig. 3 we compare the number count distributions of the *U* and *B* filters with the model predictions of Metcalfe et al. (2001) of pure luminosity evolution (short-dashed lines), pure luminosity evolution with the inclusion of a population of star-forming dwarf galaxies (long-dashed lines), and pure luminosity

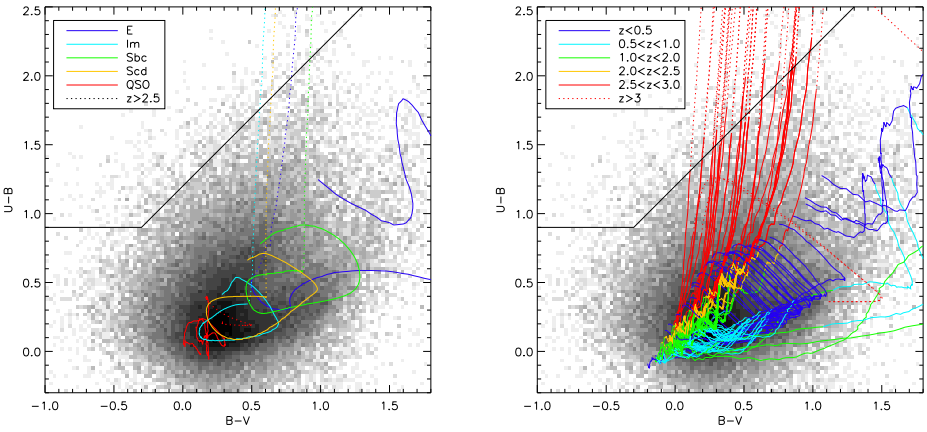

Figure 2. Optical colours of the Lockman hole sources in the AB system. The grey-scale represents the density of sources detected in all three bands are plotted. The black line marks the selection area of U-dropout sources with redshift $z \gtrsim 3$. The left panel shows the redshift tracks of the Coleman et al. (1980) templates; dotted are the tracks above $z = 2.5$, where the SEDs are not well sampled. The right panel shows the redshift tracks of SEDs created with the GISSEL98 code (Bruzual & Charlot 1993) with different metallicity and extinction properties. We use elliptical, irregular and spiral tracks, colour-coded with redshift ranges.

evolution with a steep ($\alpha = 1.75$) faint-end slope of the luminosity function. The faint-end slopes agree with the latter model for both the *U* and the *B* filters, but the counts are under-predicted for the *U*-band. A combination of the "steep faint-end slope" model with the inclusion of star-forming dwarf galaxies would better fit the data, however such a population should not affect the *B* counts, leaving a narrow redshift range for this population $2 \lesssim z \lesssim 2.5$, assuming that they are Lyman-α emitters.

Fig. 4 compares the number counts of the Lockman Hole in the *B* and *V* bands with predictions of Nagashima et al. (2005) using strong (solid lines) and weak (dashed lines) supernova feedback. The models over-predict the counts, but the faint-end slopes agree with the weak SN feedback model for the *B*-band and the strong SN feedback model for the *V*-band. This could be explained with enhanced star formation at $z \gtrsim 1.5$ where the near-UV light affects the *V* and not the *B* band.

Acknowledgments. Based on data acquired using the large binocular telescope (LBT). The LBT is an international collaboration among institutions in the United States, Italy, and Germany. LBT Corporation partners are the University of Arizona on behalf of the Arizona university system; Istituto Nazionale di Astrofisica, Italy; LBT Beteiligungsgesellschaft, Germany, representing the Max-Planck Society, the Astrophysical Institute Potsdam, and Heidelberg University; Ohio State University, and the Research Corporation, on behalf of the University of Notre Dame, the University of Minnesota, and the University of Virginia. We thank the LBT Science Demonstration Time (SDT) team for assembling and executing the SDT program. We also thank the LBC team and the LBTO staff for their kind assistance.

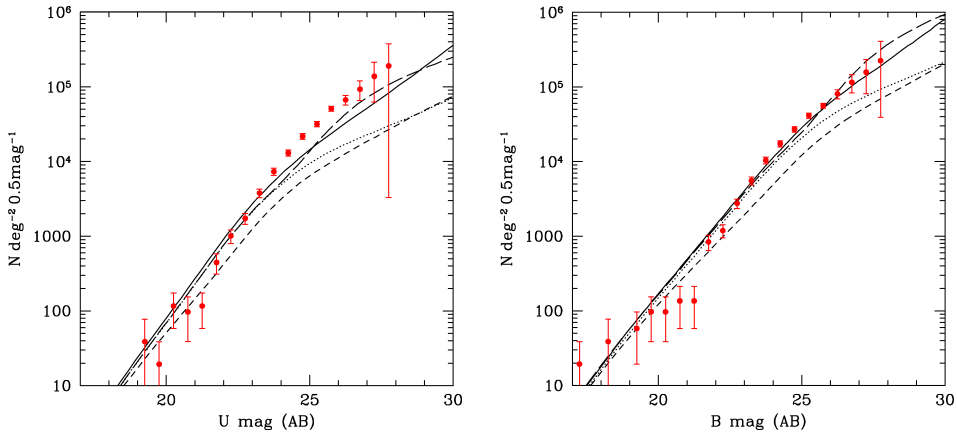

Figure 3. Measured surface densities in the U and B band (red points), plotted with evolution models from Metcalfe et al. (2001). The short-dashed lines represent the pure luminosity evolution model, the long-dashed lines the same model with the inclusion of a population of star-forming dwarf galaxies, and the solid lines the same pure luminosity evolution model with a steep faint-end slope of the luminosity function. The latter is in very good agreement with the *B*-band counts, while the *U*-band counts are under-predicted by all models.

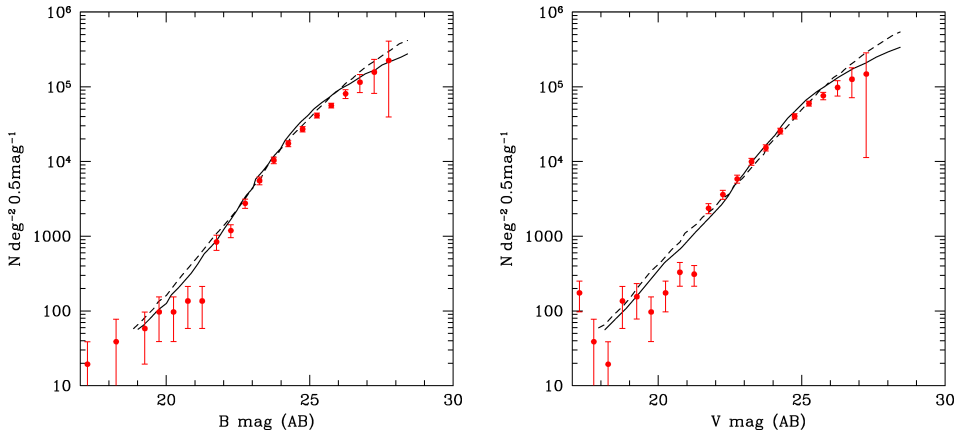

Figure 4. Measured surface densities in the B and V band (red points), plotted with number counts from the simulations of Nagashima et al. (2005). The solid and dashed lines represent the strong and weak supernova feedback cases respectively. The faint end slope of the weak feedback model is in better agreement with the *B*-band data, while the the strong feedback model is in better agreement with the *V*-band data.

References

Biggs, A. D., Ivison, R. J., 2008, MNRAS, 385, 893
Biggs, A. D., Ivison, R. J., 2006, MNRAS, 371, 963
Brunner, H., Cappelluti, N., Hasinger, G., Barcons, X., Fabian, A. C., Mainieri, V., Szokoly, G., 2008, A&A, 479, 283
Bruzual, A. G., Charlot, S., 1993, ApJ, 405, 538

Ciliegi, P., Zamorani, G., Hasinger, G., Lehmann, I., Szokoly, G., Wilson, G., 2003, A&A, 398, 901
Coleman, G. D., Wu, C.-C., Weedman, D. W., 1980, ApJS, 43, 393
Coppin, K., Chapin, E. L., Mortier, A. M. J., et al., 2006, MNRAS, 372, 1621
Egami, E., Bock, J., Dole, H., et al., 2008, sptz.prop, 50249E
Fadda, D., Lari, C., Rodighiero, G., Franceschini, A., Elbaz, D., Cesarsky, C., Perez-Fournon, I., 2004, A&A, 427, 23
Garn, T., Green, D. A., Riley, J. M., Alexander, P., 2008, MNRAS, 387, 1037
Giallongo, E, Ragazzoni, R., Grazian, A., et al., 2008, A&A, 482, 349
Greve, T. R., Ivison, R. J., Bertoldi, F., Stevens, J. A., Dunlop, J. S., Lutz, D., Carilli, C. L., et al., 2004, MNRAS, 354, 779
Hasinger, G., Burg, R., Giacconi, R., Schmidt, M., Trümper, J., Zamorani, G., 1998, A&A, 329, 482
Hasinger, G., Altieri, B., Arnaud, M., et al., 2001, A&A, 365, L45
Huang, J.-S., Barmby, P., Fazio, G. G., et al., 2004, ApJS, 154, 44
Ivison, R. J., Greve, T. R., Smail, I., et al., 2002, MNRAS, 337, 1
Kawara, K., Matsuhara, H., Okuda, H., et al., 2004, A&A, 413, 843
Lawrence, A., Warren, S. J., Almaini, O., et al., 2007, MNRAS, 379, 1599
Laurent, G. T., Aguirre, J. E., Glenn, J., et al., 2005, ApJ, 623, 742
Lockman, F. J., Jahoda, K., McCammon, D., 1986, ApJ, 302, 432
Lonsdale, C. J., Smith, H. E., Rowan-Robinson, M., et al., 2003, PASP, 115, 897
Martin, D. C., Fanson, J., Schiminovich, D., et al., 2005, ApJ, 619, L1
Metcalfe, N., Shanks, T., Campos, A., McCracken, H. J., Fong, R., 2001, MNRAS, 323, 795
Monet, D. G., 1998, AAS, 19312003
Nagashima, M., Yahagi, H., Enoki, M., Yoshii, Y., Gouda, N., 2005, ApJ, 634, 26
Rodighiero, G., Lari, C., Fadda, D., Franceschini, A., Elbaz, D., Cesarsky, C., 2004, A&A, 427, 773
Scott, K., et al., 2006, AAS, 209, 8303